# Mutagenesis of the Yeast Gene *PRP8* Reveals Domains Governing the Specificity and Fidelity of 3′ Splice Site Selection

**James G. Umen and Christine Guthrie**

*Department of Biochemistry and Biophysics, University of California, San Francisco, California 94143-0448*

Manuscript received October 13, 1995
Accepted for publication March 12, 1996

ABSTRACT

*PRP8* encodes a highly conserved U5 snRNP protein required for spliceosome assembly and later steps of pre-mRNA splicing. We recently identified a novel allele, *prp8-101,* that specifically impairs recognition of the uridine tract that precedes most yeast 3′ slice sites. We carried out extensive mutagenesis of the gene and selected for new alleles that confer a phenotype similar to that of *prp8-101.* The strongest alleles cause changes in one of two amino acids in the C-terminal portion of the protein. We also identified a second class of *PRP8* mutant that affects the fidelity of 3′ splice site utilization. These alleles suppress point mutations in the PyAG motif at the 3′ splice site and do not alter uridine tract recognition. The strongest of these alleles map to a region directly upstream of the *prp8-101*-like mutations. These new *PRP8* alleles define two separable functions of Prp8p, required for specificity of 3′ splice site selection and fidelity of 3′ splice site utilization, respectively. Taken together with other recent biochemical and genetic data, our results suggest that Prp8p plays a functional role at the active site of the spliceosome during the second catalytic step of splicing.

NUCLEAR pre-mRNA splicing involves the recognition and removal of introns from messenger RNA precursors. Introns are identified by conserved sequences at the 5′ splice site, branchsite, and 3′ splice site. These sequences are recognized by five small nuclear ribonucleoprotein particles (U1, U2, U4, U5, and U6 snRNPs) that, together with numerous accessory proteins, assemble onto intron-containing RNAs to form the spliceosome. The spliceosome catalyzes the removal of introns in two chemical steps involving 5′ splice site cleavage and branched lariat formation (step 1), followed by 3′ splice site cleavage and exon ligation (step 2) (reviewed in GREEN 1991; GUTHRIE 1991; RYMOND and ROSBASH 1992; MOORE *et al.* 1993).

A key question is how introns are accurately identified. The 5′ splice site and branchsite are recognized by a well-characterized set of interacting snRNAs and proteins (reviewed above). However, much less is known about how the 3′ splice site is identified. In most organisms, the 3′ splice site is composed of a nearly invariant PyAG motif preceding the 3′ splice junction and an upstream pyrimidine-rich tract. In mammals, the pyrimidine tract is first bound by U2AF, which is required for the first step of splicing, and later by PSF, which is required for the second step (ZAMORE and GREEN 1991; PATTON *et al.* 1993; GOZANI *et al.* 1994).

Several RNA-RNA interactions are also required for proper 3′ splice site selection. The first and last guanosine residues in introns share a non-Watson-Crick interaction that is critical for 3′ splice site utilization (PARKER and SILICIANO 1993; CHANFREAU *et al.* 1994; DEIRDRE *et al.* 1995). U5 snRNA can interact with the first two residues of the second exon and may play a role in aligning the two exons during the second step of splicing (NEWMAN and NORMAN 1992; SONTHEIMER and STEITZ 1993). Because exon sequences are poorly conserved, this interaction probably does not normally play a major role in 3′ splice site selection. Finally, mutations in U2 and U6 snRNAs can compromise the fidelity of 3′ splice site utilization and nonspecifically suppress the effects of point mutations in the PyAG motif (LESSER and GUTHRIE 1993b; MADHANI and GUTHRIE 1994). As these residues are in a domain of U2 and U6 that is thought to be part of the spliceosomal active site, their alteration may change the architecture of this region so as to relax its stringency for 3′ splice site nucleotide identity (MADHANI and GUTHRIE 1994).

We have focused on the role of a highly conserved U5 snRNP protein, Prp8p, in 3′ splice site selection (HODGES *et al.* 1995; UMEN and GUTHRIE 1995a). Prp8p was first shown to have a role in spliceosome assembly before the first catalytic step (JACKSON *et al.* 1988; BROWN and BEGGS 1992). Recently, however, we identified a novel allele, *prp8-101,* that impairs recognition of the 3′ splice site uridine-rich tract during the second catalytic step (UMEN and GUTHRIE 1995a). Consistent with a direct role in 3′ splice site recognition, Prp8p can be cross-linked to the 3′ splice site in a site-specific manner during splicing after the first catalytic step (TEIGELKAMP *et al.* 1995; UMEN and GUTHRIE 1995a). A more detailed kinetic analysis of its interaction with the 3′ splice site indicates that Prp8p is likely to be bound

*Corresponding author:* Christine Guthrie, Department of Biochemistry and Biophysics, University of California, 513 Parnassus, San Francisco, CA 94143-0448. E-mail: guthrie@cgl.ucsf.edu

to the 3′ splice site during the second catalytic event (Umen and Guthrie 1995b). However, to date, there is no functional evidence of a role for Prp8p in catalysis or in recognition of the conserved PyAG trinucleotide at the 3′ splice junction.

Although Prp8p is likely to be an RNA-binding protein, it does not contain any significant homologies to known RNA-binding proteins or other families of proteins (Hodges *et al.* 1995). Thus, there are no obvious structural domains that might be candidates for intron binding sites. In this work, we have carried out an extensive mutagenesis of the *PRP8* gene with two objectives. The first is to genetically map the domain(s) of the protein responsible for uridine tract recognition, and the second is to determine whether a domain of Prp8p interacts functionally with the PyAG trinucleotide at the 3′ splice site. We have found that all uridine recognition mutants (like *prp8-101;* Umen and Guthrie 1995a) cause alterations in the C-terminal portion of the protein. The strongest of these new alleles (including new isolates of *prp8-101*) change one of two codons. We have identified a second class of mutations that alters the fidelity of 3′ splice site utilization. These also cause alterations in the C-terminal half of Prp8, but in a region upstream of the alterations caused by the *prp8-101*-like class. Unlike *prp8-101,* which exacerbates the effects of point mutations in the PyAG motif at the 3′ splice junction (Umen and Guthrie 1995a), this class of *PRP8* mutant suppresses the effects of PyAG alterations. The complex spectrum of preferences for different PyAG alterations displayed by these *PRP8* alleles is suggestive of a direct interaction between Prp8p and the PyAG trinucleotide and/or the spliceosomal active site.

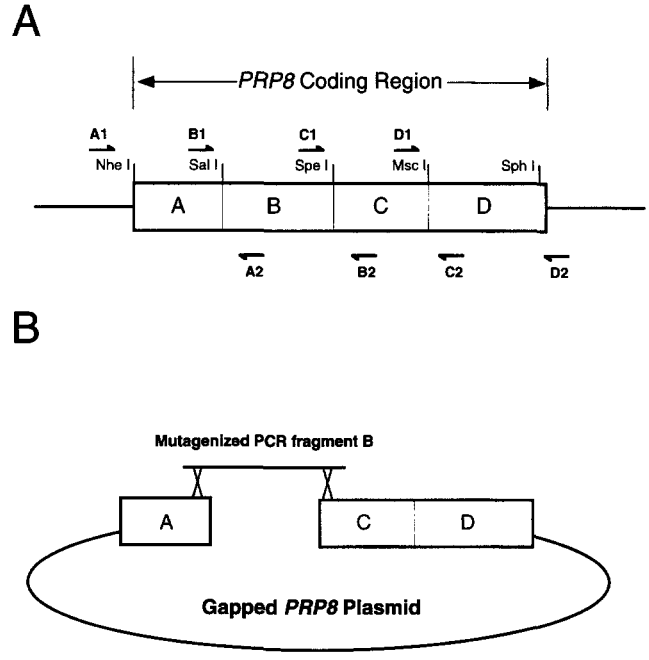


Figure 1.—Strategy for isolation of novel *PRP8* mutants. (A) Schematic of *PRP8* gene with locations of PCR primers (depicted as arrows) and restriction sites in their approximate locations (see Materials and Methods for details). (B) Example of *in vivo* gap repair used to generate mutant library from PCR fragment B. The ends of this fragment are shown recombining with a gapped *PRP8* plasmid cut with *Sal*I and *Spe*I. (C) Depicted is a yeast cell containing a reporter construct, wild-type *PRP8* gene and selectively mutagenized *PRP8* gene (region B from above). The strain is deleted for its chromosomal copy of *PRP8* and *CUP1*. *PRP8* mutants that affect splicing of the reporter construct can be selected before or after loss of the wild-type *PRP8* allele by 5FOA selection.

## MATERIALS AND METHODS

**Yeast methods:** All methods for manipulation of yeast, including media preparation, growth conditions, transformation, plasmid recovery and 5-fluoro-orotic acid (5FOA) selection were performed according to standard methods (Guthrie and Fink 1991). Copper growth assays and β-galactosidase assays were performed as previously described (Miller 1972; Lesser and Guthrie 1993a). Strains for β-galactosidase assays were grown in media containing 2% galactose and 2% raffinose for 24 h before analysis in order to induce expression of the lacZ fusion construct. Strain YJU75 (with various plasmids described below) was used for all experiments: *MAT***a** *ade 2 cup1*Δ*::ura3 his3 leu2 lys2 prp8*Δ*::LYS2 trp1* pJU169 (*PRP8 URA3 CEN ARS*). Disruption of the *PRP8* locus is described below.

After mutagenesis and transformation, 3′ splice site selection mutants were selected by replica plating to copper-containing plates before or after replica plating to 5FOA-containing plates.

**Plasmid construction:** Molecular cloning procedures were carried out according to standard methods (Maniatis *et al.* 1982). Plasmid pJU225 (*PRP8 TRP1* 2μ) was constructed from a previously described plasmid JDY13 (*GAL::PRP8*) (Brown and Beggs 1992). The galactose-driven promoter in this plasmid was removed by cutting with *Nhe*I and *Xho*I. A wild-type copy of the promoter was amplified by PCR under nonmutagenic conditions and used to replace the galactose driven promoter. The entire *PRP8* gene was then excised using *Xho*I and *Not*I and ligated to plasmid RS424 (*TRP1* 2μ) also cut with *Xho*I and *Not*I (Sikorski and Hieter 1989).

For all nonmutagenic PCR reactions, Hot Tub polymerase (Amersham) was used according to the manufacturer's instructions.

The 2.1 kb *Bst*EII fragment from pJU225 was swapped between wild type and mutant clones using standard procedures. The chimeras were confirmed by sequencing the relevant regions.

*ACT1-CUP1* reporters are depicted in Figure 2. The 3′ splice site competition reporters and construct set II were made according to previously described methods (Umen and Guthrie 1995a). Construct set I plasmids were made by using oligonucleotide directed mutagenesis. The sequences that were altered compared to the standard *ACT1-CUP1* fusion are depicted.

The *ACT1-CUP1* G5A reporter with either the normal (NI) or cryptic (Ab) 5′ cleavage sites in frame with the *CUP1* coding sequence were constructed by Amy Kistler. The *rp51a-lacZ* fusion construct and *ACT1-CUP1* A259C construct have been described previously (Lesser and Guthrie 1993a; Chanfreau *et al.* 1994).

The *prp8*Δ*::LYS2* disruption plasmid was constructed by first eliminating the *Not*I site in the polylinker region of pJU225. A *Not*I site was then introduced into the 5′ end of *PRP8* at the fifth codon using PCR-based mutagenesis. A 4-kb fragment containing the *LYS2* gene in the polylinker of a Bluescript plasmid (Stratagene) was excised with *Not*I and *Cla*I and ligated to the *Cla*I and *Not*I sites of the modified

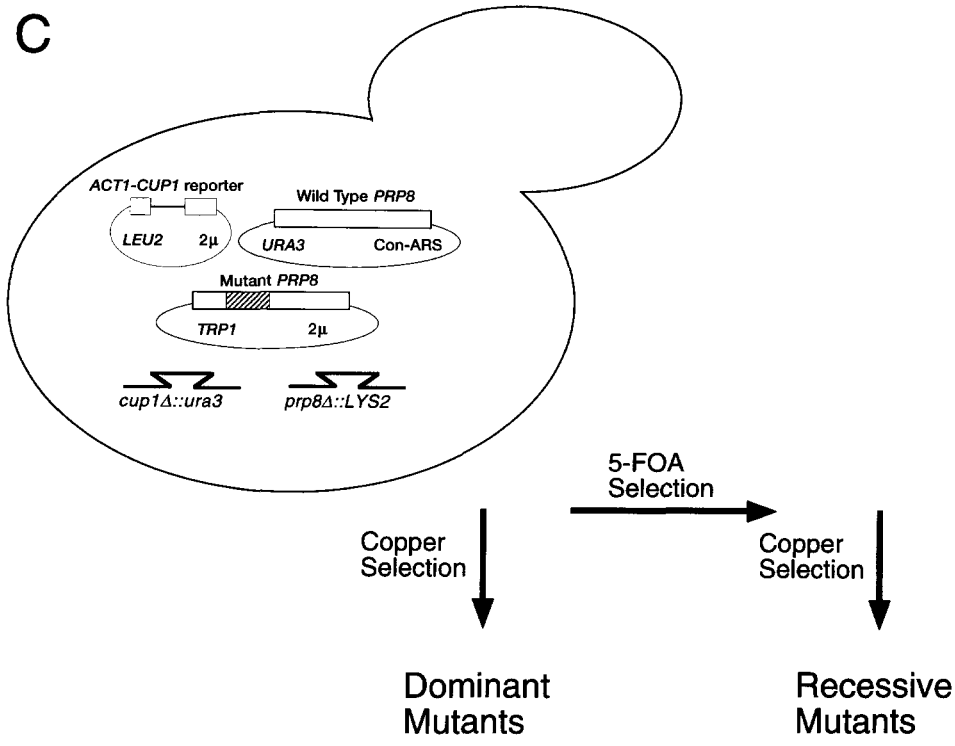


FIGURE 1.—Continued

*PRP8* plasmid just described. This disruption removes all but the first five and last four codons of *PRP8*.

To generate strain YJU75, the *prp8Δ::LYS2* fragment with *PRP8* flanking sequence (1–2 kb on each side) was excised from the disruption plasmid with *Sac*I and *Apa*I and transformed into strain L5 (UMEN and GUTHRIE 1995a), which contained plasmid pJU169 (*PRP8 URA3 CEN ARS*). $Lys^+$ transformants were screened for disruption of the chromosomal *PRP8* locus by their inability to grow on 5FOA-containing media. The disruption was confirmed by a whole cell PCR assay, and the 5FOA induced lethality was rescued by the presence of a non-*URA3*-marked *PRP8* plasmid (data not shown).

**PCR mutagenesis:** The strategy we used for mutagenic PCR is described in Figure 1 (MUHLRAD *et al.* 1992). Mutagenic PCR conditions have been described previously (LEUNG *et al.* 1989). Primer sequences and $Mn^{2+}$ concentrations were as follows: A1, 5′-GCATGCTCGAGACTTCAAAGCATGG-3′; A2, 5′-ACATGCGCGGATTTGATGCAT-3′, 0.1 mM $MnCl_2$; B1, 5′-AATACAAAAGATGCGATGTCG-3′; B2, 5′-GCTCGCCCTAGGTTAACGTCC-3′, 0.03 mM $MnCl_2$; C1, 5′-CAGAGATACCACCTCTTCTGG-3′; C2, 5′-TAGAAAATGCAGTGTACGATG-3′, 0.05 mM $MnCl_2$; D1, 5′-TGATCGGTATCGATTTGGCT-3′; and D2, 5′-CTAAATACATCGATTTGTTCG-3′, 0.1 mM $MnCl_2$. When $MnCl_2$ was included, 200 μM dATP, 1 mM dGTP, dTTP and dCTP were used. Without $MnCl_2$, all dNTPs were used at 1 mM.

PCR reaction volumes were performed in 4 × 50 μl aliquots using Amplitaq polymerase (Perkin-Elmer). The samples were then extracted with phenol/chloroform and precipitated with 0.4 volumes 3 M NaOAc (80 μl) and 1.4 volumes isopropanol (280 μl). The appropriate PCR product was cotransformed with gapped plasmid pJU225, with the PCR DNA in a mass ratio of 5 PCR DNA:1 vector DNA. The enzymes used for gapping pJU225 were: (A) *Nhe*I/*Sal*I, (B) *Sal*I/*Spe*I, (C) *Spe*I/*Msc*I, (D) *Msc*I/*Sph*I.

**Gap repair:** To determine whether the mutations we identified were necessary and sufficient to generate the phenotypes we observed, regions of a mutant (or wild-type control) plasmid were amplified using nonmutagenic PCR conditions (see above) and cotransformed with gapped wild-type vector (pJU225). For *prp8-101–prp8-107*, the amplified region spanned nucleotides 5322–6024 of the coding region, and the vector was cut with *Msc*I at position 5723. For *prp8-121–prp8-125*, the amplified region spanned nucleotides 4125–5322 of the coding sequence, and the vector was partially digested with *Bst*EII in the presence of 100 μg/ml ethidium bromide (EtBr). The EtBr enriched for singly cut plasmids. The relevant cut site that can be repaired from the PCR DNA is at nucleotide 4829 of the coding region. The other *Bst*EII site is at nucleotide 6931. In each case, the mutant PCR DNA stimulated the appearance of a mutant phenotype by 10- to 1000-fold over amplified wild-type DNA.

**RNA analysis:** RNA preparation and primer extensions assays were performed as previously described (LESSER and GUTHRIE 1993a). Results were quantitated by phosphorimager scanning of duplicate or triplicate samples.

## RESULTS

**Mutagenesis strategy for *PRP8*:** To identify new alleles of *PRP8*, we utilized PCR, which can efficiently mutagenize a selected region of DNA (LEUNG *et al.* 1989; MUHLRAD *et al.* 1992). Since the coding region of *PRP8* is very large (7.2 kb), we divided the gene into four approximately equal-sized regions (A–D) based on convenient restriction sites (Figure 1). This division was necessary to reduce the high frequency of null alleles that would be expected if the whole coding region were mutagenized simultaneously, and it also facilitated the mapping of mutations. Each region of the gene was amplified using Taq polymerase, with and without added manganese. Manganese has been reported to increase the error rate of Taq polymerase by approximately fivefold (LEUNG *et al.* 1989). Each PCR fragment

**TABLE 1**

**Characterization of mutagenized *PRP8* library**

| Mutagenized region | No. of transformants | Percentage null | No. of temperature-sensitive/50 | Percentage *prp8-101*-like[a] | Percentage 3′ splice site suppressors[a] |
|---|---|---|---|---|---|
| Gap A | ~500 | 4 | ND | ND | ND |
| +PCR A | ~4000 | 18 | ND | 0 (0) | 0 (0) |
| +PCR A + $Mn^{2+}$ | ~4000 | 76 | ND | 0 (0) | 0 (0) |
| Gap B | ~800 | 4 | 0 | ND | ND |
| +PCR B | ~4000 | 34 | 0 | 0 (0) | .025 (1) |
| +PCR B +$Mn^{2+}$ | ~4000 | 48 | 9 | 0 (0) | .025 (1) |
| Gap C | ~800 | 4 | 0 | ND | ND |
| +PCR C | ~4000 | 40 | 2 | .4 (16) | .2 (8) |
| +PCR C +$Mn^{2+}$ | ~4000 | 64 | 1 | .075 (3) | .1 (4) |
| Gap D | ~800 | 8 | 0 | ND | ND |
| +PCR D | ~4000 | 32 | 3 | .55 (22) | .13 (5) |
| +PCR D +$Mn^{2+}$ | ~4000 | 62 | 5 | .1 (4) | 0 (0) |

The first column indicates the region of the gene that was mutagenized (Gap A–D) and cotransformed alone or with PCR DNA (+PCR A–D) or with manganese mutagenized PCR DNA (+PCR +$Mn^{2+}$ A–D). The second column indicates the number of transformants screened and the third column indicates the percentage null alleles generated (scored as inviable on 5FOA-containing media). The fourth column indicates the number of temperature-sensitive mutants obtained from 50 randomly chosen transformants. The fifth column indicates the percentage of transformants with a *prp8-101*-like phenotype (loss of uridine recognition) with the actual number isolated indicated in parentheses. The last column indicates the percentage of transformants that suppress 3′ GAG (described in text) with the actual number isolated indicated in parentheses. ND, parameter was not assayed.

[a] Values in parentheses are total number isolated.

was cotransformed into a recipient strain along with an appropriately gapped, high copy *PRP8* plasmid. Since the PCR fragments contained ~300 nucleotides of homology on each side of the gapped region, they could direct repair of the gapped *PRP8* plasmid (Figure 1B) (MUHLRAD *et al.* 1992). When no PCR-amplified DNA is cotransformed with the gapped plasmid, the gap can be repaired efficiently from the plasmid-borne copy of *PRP8* that is already in the cell (Table 1; see below). However, based on the frequencies of null mutants obtained in the presence of PCR-amplified DNA, the PCR DNAs appear to compete strongly as repair donors, probably because they contain free ends. The PCR DNA also stimulated transformation efficiency approximately fivefold (data not shown).

The transformants were initially scored in several assays. Each recipient strain contained a low copy, *URA3*-marked plasmid bearing the wild-type *PRP8* gene and a high copy, *LEU2*-marked plasmid bearing an *ACT1-CUP1* gene fusion as a splicing reporter. By selecting against cells harboring the wild-type *PRP8* plasmid with 5FOA, the recessive phenotypes of the *PRP8* mutants could be determined (Figure 1C). As a measure of mutagenic efficiency, we scored null alleles by their inability to grow on 5FOA-containing plates. Without cotransformation of PCR DNA, the null frequency was low for each gapped region (4–8%). Cotransformation of PCR DNA caused a four- to 10-fold increase in the frequency of null alleles, and the use of manganese mutagenized PCR DNA caused a further increase to a null frequency of 48–76%. We also screened a limited number of mutants (300 total in six separate pools; see Table 1) for temperature or cold sensitivity after selection on 5FOA. Although the number of transformants scored this way was too low to be statistically significant, we found a surprisingly large number of temperature-sensitive *PRP8* mutants (20/300). These were distributed among the three regions that we scored: B–D. We did not recover any cold-sensitive mutants. In summary, the mutagenesis strategy that we have developed efficiently targets four different subregions of *PRP8* and allows rapid identification of alleles that confer different splicing phenotypes (Table 1; see below).

**Identification of new *prp8-101*-like alleles:** To identify new alleles of *PRP8* that affect uridine tract recognition, we introduced the eight pools of our library (A–D, $\pm MnCl_2$) into a recipient strain harboring the reporter ACT-CUP +T PyDOWN (Figure 2A). The reporter directs synthesis of an intron-containing RNA with duplicated 3′ splice sites, one uridine-rich and the other adenosine-rich. The intron is fused to the *CUP1* gene, which encodes a copper-chelating metallothionein homologue that can be used as a selectable marker (LESSER and GUTHRIE 1993a). Use of the branchsite-proximal, uridine-rich 3′ splice site produces a message where the initiator AUG in exon one is out of frame with the *CUP1* coding sequence, whereas use of the branchsite-distal, adenosine-rich 3′ splice site results in the initiator codon being in frame with *CUP1* (PATTERSON and GUTHRIE 1991; UMEN and GUTHRIE 1995a). In wild-type strains, the uridine-rich 3′ splice site is preferred >20:1 over the adenosine-rich competitor (Fig-


FIGURE 2.—3′ splice site reporter constructs. (A) 3′ splice site competition constructs. The sequence between the branchsite (raised A in bold) and two competing 3′ splice sites (underlined and bold AGs) is shown. (B) Reporter set I. As above with mutated splice acceptor sequence in bold and cleavage site followed by a / symbol. Exon 2 sequences that have been altered are also shown. (C) Reporter set II. As in (B) except only the wild-type version is shown in its entirety with mutants at the 3′ acceptor sequence drawn below. The cryptic UG splice acceptor is also underlined.

ure 3A, lane 2; Table 2). Loss of uridine recognition and the consequent activation of the adenosine-rich 3′ splice site generates more in-frame message and Cup1 fusion protein. Since the chromosomal copy of *CUP1* is deleted in this strain, we can detect increased splicing to the adenosine-rich 3′ splice site by measuring increased copper resistance (LESSER and GUTHRIE 1993a; UMEN and GUTHRIE 1995a).

The wild-type strain harboring +T PyDOWN cannot survive at copper concentrations above 0.05 mM while the *prp8-101* mutant allows growth at 0.18–0.25 mM copper (UMEN and GUTHRIE 1995a). The pools of trans-

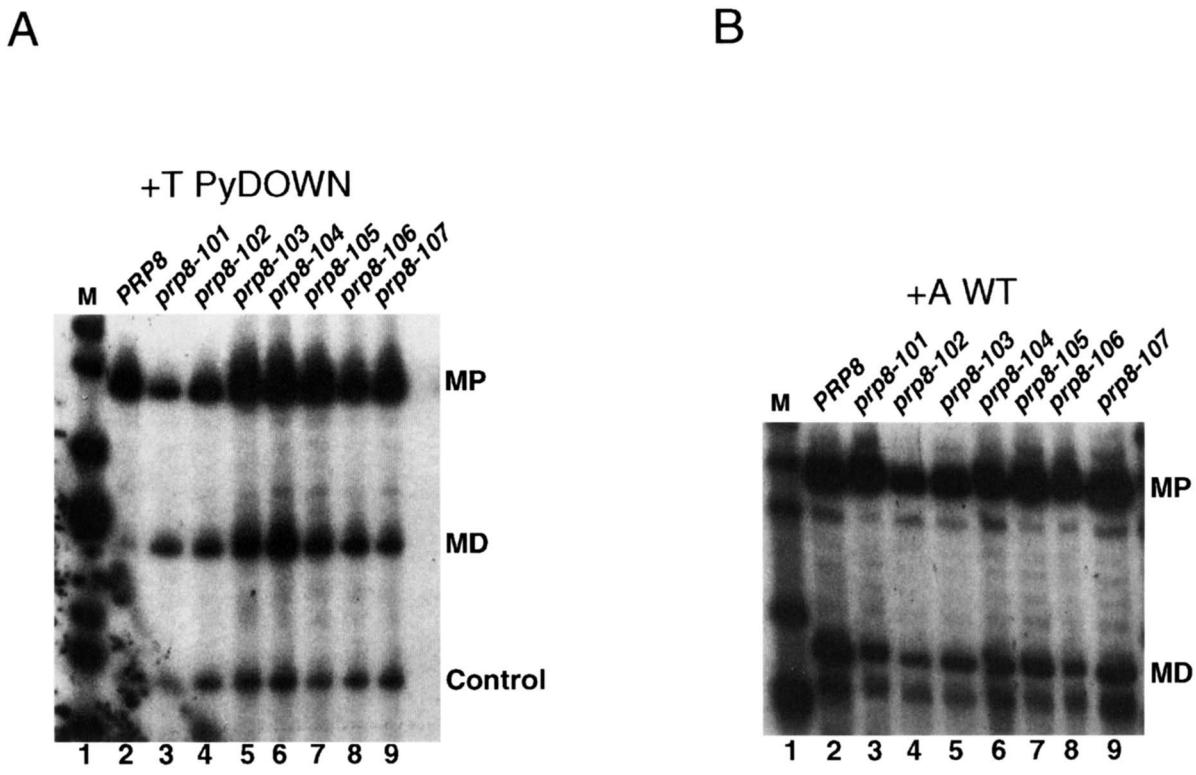


FIGURE 3.—Splicing of 3′ splice site competition constructs. (A) Primer extension analysis of +T PyDOWN splicing in wild-type (lane 2) and *prp8-101–prp8-107* strains (lanes 3–9). Primer extension products corresponding to mature message from use of the branchsite proximal (MP) and branchsite distal (MD) 3′ splice sites are marked next to the bands. A U1 snRNA primer extension product (control) is used as an internal control. Lane 1 (marked M) contains size markers (*Hpa*II-digested pBR325). (B) Splicing of +A WT. Lanes and primer extension products are marked as in (A). The internal control band is not shown.

**TABLE 2**

**Phenotypes of new *prp8-101*-like alleles**

| Allele | RNA | Primer extension analysis | | Copper resistance (mM) |
|---|---|---|---|---|
| | | MP/MD | Loss of uridine preference | |
| *PRP8* | +T PyDOWN | 26 | NA | 0.05 |
| *prp8-101* | +T PyDOWN | 2.0 | 13× | 0.18 |
| *prp8-102* | +T PyDOWN | 4.9 | 5.3× | 0.15 |
| *prp8-103* | +T PyDOWN | 3.6 | 7.2× | ±0.15 |
| *prp8-104* | +T PyDOWN | 3.1 | 8.4× | 0.18 |
| *prp8-105* | +T PyDOWN | 5.2 | 5.0× | ±0.13 |
| *prp8-106* | +T PyDOWN | 2.2 | 12× | 0.15 |
| *prp8-107* | +T PyDOWN | 5.3 | 4.9× | 0.15 |
| *PRP8* | +A WT | 2.3 | NA | ND |
| *prp8-101* | +A WT | 7.4 | 3.2× | ND |
| *prp8-102* | +A WT | 6.5 | 2.8× | ND |
| *prp8-103* | +A WT | 3.7 | 1.6× | ND |
| *prp8-104* | +A WT | 5.1 | 2.2× | ND |
| *prp8-105* | +A WT | 7.9 | 3.4× | ND |
| *prp8-106* | +A WT | 7.6 | 3.3× | ND |
| *prp8-107* | +A WT | 3.9 | 1.7× | ND |

The first column indicates the *PRP8* allele assayed. The second column indicates the reporter construct that was utilized. The third column shows quantitation of primer extension data as the ratio of branchsite proximal (MP) to branchsite distal (MD) mRNA from each of the competing 3′ splice sites from Figure 3. The fourth column represents the amount of uridine preference lost in each mutant. For +T PyDOWN this value is (MP/MD)wild type/(MP/MD)mutant. For +A WT this value is (MP/MD)mutant/(MP/MD)wild type. The last column represents maximum copper resistance of each strain with the branchsite distal 3′ splices site (uridine poor 3′ splice site for +T PyDOWN) in frame with the *CUP1* sequence. NA, not applicable; ND, parameter was not measured.

formants were replica plated to copper concentrations ranging from 0.1 to 0.5 mM either before or after selection on 5FOA. No cells transformed with the A and B libraries grew at or above 0.1 mM in this assay, indicating that it is difficult or impossible to mutate regions A and B and obtain a *prp8-101*-like phenotype. We obtained a combined total of 45 presumptive dominant isolates that grew at or above 0.1 mM copper before FOA selection from cells transformed with the C and D libraries. The *prp8-101* mutation lies in an overlap region of the C and D libraries and could, in principle, be obtained from either pool (Umen and Guthrie 1995a). After selection on 5FOA, there were ~100 additional presumptive recessive isolates that could grow at or above 0.1 mM copper (Table 1). As we were interested in the strongest alleles, we focused on 12 isolates that grew at the highest copper concentrations (0.15–0.25 mM) before 5FOA selection.

By transformation into *Escherichia coli,* we were successful in rescuing the mutant *PRP8* plasmids from 11 of the 12 isolates. These clones, which were later found to represent seven different alleles of *PRP8, prp8-101–prp8-107,* were retransformed into the original yeast strain harboring the reporter plasmid +T PyDOWN, and each was retested for the *prp8-101*-like phenotype by growth on copper-containing media. Like *prp8-101,* each new mutant conferred increased copper resistance in the presence of the wild-type *PRP8* plasmid but showed slightly higher copper resistance after selection of 5FOA (Table 2, data not shown). Thus, these alleles are all haploviable and semidominant.

To directly test the effect of the new alleles on alternative splice site selection, we analyzed RNA isolated from mutant and wild-type strains by primer extension. In wild-type cells, the ratio of branchsite-proximal uridine-rich 3′ splice site usage *vs.* branchsite-distal, adenosine-rich 3′ splice site is 26:1. In all mutant strains, splicing to the distal splice site is activated and the ratio of splice site usage is more balanced (Figure 3A, lane 2 *vs.* lanes 3–9; Table 2). *prp8-101* and *prp8-106* display the largest change in this ratio (2.0:1 and 2.2:1). The copper resistance does not correlate strictly with the primer extension data because the mutations cause two phenotypes. The first phenotype is activation of the distal splice site, which increases copper resistance, and the second is an overall decrease in the efficiency of splicing, which tends to reduce levels of both the proximal and distal mature messages and decrease copper resistance. Thus, in *prp8-106,* the overall efficiency of splicing is slightly reduced in comparison with *prp8-101.*

We also examined splicing with a different 3′ splice site competition construct, +A WT (Figure 2A; Patterson and Guthrie 1991; Umen and Guthrie 1995a). The RNA produced from this plasmid differs from that of +T PyDOWN in that the branchsite-proximal 3′ splice site is adenosine-rich and the branchsite-distal 3′ splice site is uridine-rich. The reversed order of the 3′ splice sites in this construct *vs.* +T PyDOWN allows us

to rule out differences in distance or spacing preference as the cause of the phenotype. With +A WT, the change in ratios of 3′ splice site usage in the mutant strains is again altered to reduce splicing to the uridine-rich 3′ splice site (Figure 3B, lane 2 *vs.* lanes 3–9; Table 2). Thus, the change in ratio of splice site usage in the mutant strains, with both +T PyDOWN and +A WT, correlates with the placement of the uridine-rich tract and not with the relative positions of the competing splice sites. This result confirms that the new mutants are all impaired in uridine tract recognition *per se.*

**Mapping uridine recognition mutations:** To determine the nature and location of the mutations in these new alleles, we sequenced the region of overlap between the C and D libraries in each clone. We reasoned that this would be a likely location for the relevant mutations since it is where the original *prp8-101* mutation lies. Among the 11 isolates, there were two that contained the E1960K alteration found in *prp8-101.* There were three additional isolates that changed this amino acid to a G. This allele is designated *prp8-102.* The other isolates all caused a change in amino acid F1834 to L or to S. Two of the alleles, *prp8-106* and *prp8-107* only cause a change in amino acid 1834, whereas *prp8-103, prp8-104,* and *prp8-105* cause a change at 1834 and one additional alteration (Table 7; Figure 7).

That we repeatedly identified changes in the same two amino acids suggests that the mutations affecting these positions are sufficient to cause the *prp8-101*-like phenotype. To test this idea, we amplified the region we had sequenced from each clone using PCR under nonmutagenic conditions and cotransformed the amplified DNA with a wild-type *PRP8* plasmid that had been cut with *Msc*I. The *Msc*I recognition site lies in the middle of the region that we amplified for each clone and stimulates gene conversion from the amplified sequences to the plasmid. Whereas amplified wild-type *PRP8* DNA generated a very low frequency of *prp8-101*-like phenotypes upon cotransformation (<1%), cotransformed DNA amplified from the mutant alleles gave rise to a mutant phenotype at a high frequency (10–40%) (data not shown). Thus, the alterations in amino acids 1960 and 1834 are sufficient to generate the *prp8-101*-like phenotype. The additional changes in *prp8-103, prp8-104,* and *prp8-105* may slightly alter the phenotype (see Table 2) but are not necessary to confer it. Interestingly, the additional changes in these alleles occur in conserved amino acids (Figure 7) (Hodges *et al.* 1995). Despite this conservation, the identity of these residues must not be critical for the function of Prp8p.

**Isolation of 3′ splice site fidelity mutants:** There is mounting evidence that Prp8p may be present at or near the active site of the spliceosome during the second catalytic step (Teigelkamp *et al.* 1995; Umen and Guthrie 1995a,b). Therefore, we wished to test whether Prp8p plays a functional role in recognition of the PyAG trinucleotide sequence at the 3′ splice junction. Our strategy was to screen for alleles of *PRP8* that suppress the phenotypes of point mutations in the PyAG motif. The reporter constructs we used (Figure 2B, Set I) contain the sequence GAG (3′ GAG) or UUG (3′ UUG) at the 3′ splice junction. In addition, parts of exon two were altered to eliminate possible cryptic 3′ splice sites, and in 3′ UUG, two nucleotides of the intron near the 3′ splice site were fortuitously deleted during its construction. 3′ GAG confers a copper resistance of 0.1 mM; 3′ UUG confers a resistance of 0.05 *vs.* 2 mM for a wild-type 3′ splice site (Table 3; Table 4).

Mutagenized *PRP8* libraries were introduced into strains harboring one of these two constructs and transformants were selected for growth on 0.25–1 mM copper before and after 5FOA selection against the wild-type *PRP8* plasmid (Figure 1). For each construct, we isolated ~15–20 suppressors, distributed in regions B–D, that grew above 0.25 mM copper prior to 5FOA selection. The majority of suppressors arose from region C and the strongest suppressors were also from the C region. After 5FOA selection, several dozen weaker suppressors were isolated but were not characterized further. Again, the majority of these were in the C region (Table 1).

We chose six of the strongest suppressors (three for each 3′ splice site mutation), and were able to recover five of the mutant plasmids by transformation into *E. coli.* Each plasmid conferred suppression upon retransformation into yeast. These alleles are designated *prp8-121–prp8-125.* The level of suppression on copper is very high for these mutants, reaching 15-fold over wild type for those selected against 3′ UUG (*prp8-121* and *prp8-122*) and 7.5–10-fold over wild type for those selected against 3′ GAG (*prp8-123–prp8-125*) (Table 3). Each of the alleles is dominant and haploviable (data not shown).

**Specificity for suppression of 3′ splice site mutations:** We first tested whether these alleles could suppress mutations in other parts of the intron and whether they altered 3′ splice site uridine tract recognition, similar to *prp8-101–prp8-107.* We examined splicing of constructs containing a mutation in the branch nucleotide from A to C (A259C) and a construct containing a G to A mutation at the fifth position of the intron (G5A). For G5A, we measured splicing to both the authentic 5′ splice site and to an upstream cryptic 5′ splice site at position −5, which is activated by the G5A mutation (Parker and Guthrie 1985; Lesser and Guthrie 1993b). Finally, we measured splicing in the 3′ splice site competition construct +T PyDOWN. We assayed splicing of these *ACT1-CUP1* fusions by growth on copper-containing media.

Splicing of A259C is unaffected in *prp8-124* and decreased twofold in *prp8-121, -122, -123,* and *-125* (Table 4). Normal splicing of G5A is unaffected in strain *prp8-123* and decreased between two and greater than fivefold in *prp8-121, prp8-122* and *prp8-124.* We see a very slight suppression in *prp8-125* (less than twofold). For aberrant splicing of G5A, we see a similar pattern except

**TABLE 3**

**3′ splice site suppression with construct set I**

| | | Primer extension analysis | | Copper growth | |
|---|---|---|---|---|---|
| Strain | RNA | M/LI | Fold suppression | Copper growth (mM) | Fold suppression |
| *PRP8* | 3′ GAG | 0.66 | NA | 0.1 | NA |
| *prp8-121* | 3′ GAG | 3.5 | 5.3× | .25 | 2.5× |
| *prp8-122* | 3′ GAG | 3.9 | 5.9× | .25 | 2.5× |
| ***prp8-123*** | **3′ GAG** | 8.5 | 13× | .75 | 7.5× |
| ***prp8-124*** | **3′ GAG** | 5.8 | 8.8× | .75 | 7.5× |
| ***prp8-125*** | **3′ GAG** | 10.1 | 15× | .75 | 7.5× |
| *PRP8* | 3′ UUG | 0.64 | NA | .05 | NA |
| ***prp8-121*** | **3′ UUG** | 7.1 | 11× | .75 | 15× |
| ***prp8-122*** | **3′ UUG** | 5.3 | 8.3× | ±0.75 | 15× |
| *prp8-123* | 3′ UUG | 1.3 | 2.0× | .25 | 5× |
| *prp8-124* | 3′ UUG | 2.1 | 3.3× | .25 | 5× |
| *prp8-125* | 3′ UUG | 0.78 | 1.2× | .18 | 4× |

The first column indicates the strain used. The second column indicates the 3′ splice site reporter from construct set I that each strain contained. In bold is each *PRP8* allele and the 3′ splice site mutant against which it was selected. The third and fourth column represent quantitation of primer extension experiments measuring the efficiency of the second step as the ratio of mature message (M) to lariat intermediate (LI). Fold suppression is the fold increase in M/LI in the mutant *vs.* wild-type strains. The fifth and sixth columns represent copper resistance of each strain and the fold increase in copper resistance for each mutant *vs.* wild type. NA, applicable.

that *prp8-125* splices to the aberrant site at a similar level as wild type and *prp8-123* slightly suppresses aberrant splicing. Again, this suppression (less than twofold) is very slight compared with the suppression this allele confers to introns with PyAG mutations (Table 4). Finally, uridine tract recognition is unaffected by *prp8-121–prp8-125* since +T PyDOWN splicing is unchanged in these strains (Table 4). In summary, the strong suppression phenotype of alleles *prp8-121–prp8-125* appears to be specific for PyAG mutations at the 3′ splice site. Other alterations in the intron are either relatively unaffected or exacerbated by these alleles.

**TABLE 4**

**Specificity of 3′ splice site suppressors**

| Strain | RNA | Copper growth (mM)/ β-gal units | Strain | RNA | Copper growth (mM)/ β-gal units |
|---|---|---|---|---|---|
| *PRP8* | G5A Nl | ±0.25 | *PRP8* | +T PyDown | 0.05 |
| *prp8-121* | G5A Nl | <0.05 | *prp8-121* | +T PyDown | 0.05 |
| *prp8-122* | G5A Nl | <0.05 | *prp8-122* | +T PyDown | 0.05 |
| *prp8-123* | G5A Nl | 0.25 | *prp8-123* | +T PyDown | 0.05 |
| *prp8-124* | G5A Nl | 0.1 | *prp8-124* | +T PyDown | 0.05 |
| *prp8-125* | G5A Nl | 0.25 | *prp8-125* | +T PyDown | 0.05 |
| *PRP8* | G5A Ab | 0.25 | *PRP8* | rp51a 3′ UGG | 1.0 |
| *prp8-121* | G5A Ab | <0.05 | *prp8-121* | rp51a 3′ UGG | 3.5 |
| *prp8-122* | G5A Ab | <0.05 | *prp8-122* | rp51a 3′ UGG | 10 |
| *prp8-123* | G5A Ab | 0.25 | *prp8-123* | rp51a 3′ UGG | 1.2 |
| *prp8-124* | G5A Ab | 0.05 | *prp8-124* | rp51a 3′ UGG | 1.9 |
| *prp8-125* | G5A Ab | 0.25 | *prp8-125* | rp51a 3′ UGG | 15 |
| *PRP8* | A259C | 0.18 | | | |
| *prp8-121* | A259C | 0.1 | | | |
| *prp8-122* | A259C | 0.1 | | | |
| *prp8-123* | A259C | 0.1 | | | |
| *prp8-124* | A259C | 0.18 | | | |
| *prp8-125* | A259C | 0.1 | | | |

The first column indicates the strain used and the second column indicates the reporter constructs. G5A Nl and G5A Ab indicate normal and aberrant splice sites are in frame with *CUP1* in this 5′ splice site mutant. A259C is a branch site mutant and +T PyDOWN is described in Figure 2 and the legend for Table 2. rp51a 3′ UGG is described in the text. Column 3 represents maximum copper resistance for each mutant or, in the case of rp51a 3′UGG, β-galactosidase activity in arbitrary units. ±, weak growth at that concentration of copper.

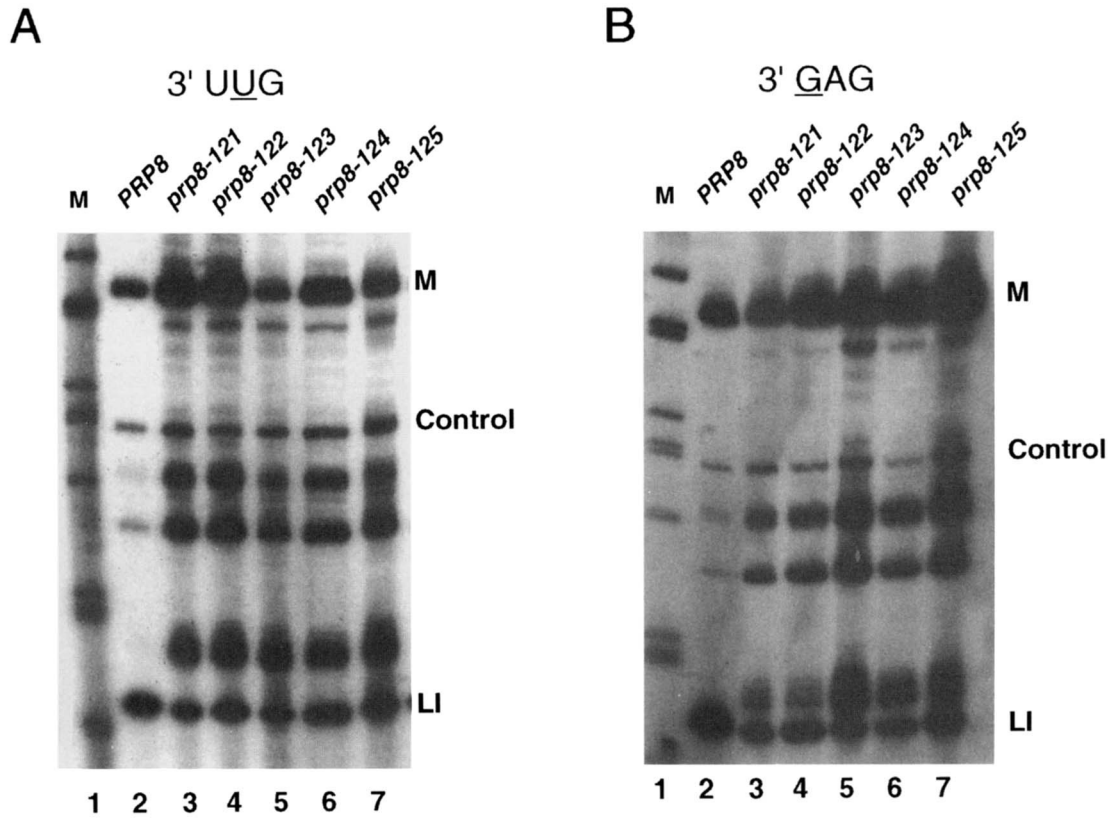


FIGURE 4.—Splicing of 3′ splice site mutant construct set I. (A) Primer extension analysis of splicing to 3′ splice site mutant UUG in wild-type (lane 2) and *prp8-121–prp8-125* (lanes 3–7) strains. Primer extension products corresponding to mature message (M) lariat intermediate (LI) and U1 snRNA internal control (control) are labeled next to gel. Other bands are strong stops that occur variably in different lanes and experiments. Lane 1 (marked M) contains size markers (*Hpa*II-digested pBR325). (B) Primer extension analysis of splicing to 3′ splice site mutant GAG. Lanes and primer extension products are marked as in (A).

**Allele specificity for different PyAG mutations:** *Construct set I (3′ GAG and UUG):* As a first test of allele specificity for different PyAG alterations, we transformed *prp8-121* and *prp8-122* into a strain harboring the 3′ GAG construct, and *prp8-123–prp8-125* into a strain harboring the 3′ UUG construct. This experiment revealed that either set of alleles could suppress a different 3′ splice site mutation other than the one it was selected against, but less efficiently. This observation was confirmed by directly analyzing splicing in mutant and wild-type strains by primer extension (Figure 4, A and B, lane 2 *vs.* lanes 3 and 4 and 5–7; Table 3). In this and in subsequent primer extension experiments, we determined the ratio of mRNA (M) to lariat intermediate (LI) as a measure of suppression. This ratio was used because 3′ splice site mutations in yeast affect only the second catalytic step, and the M/LI ratio represents the overall rate of the second catalytic step *in vivo* (PIKIELNY and ROSBASH 1985; FRANK and GUTHRIE 1992). By copper and primer extension assays, *prp8-121–prp8-125* suppress both types of 3′ splice site mutations but exhibit some allele preference (Table 3).

*Construct set II (3′ UAG, AAG, GAG and UGG):* To better characterize the effects of *prp8-121–prp8-125* on 3′ splice site utilization, we tested a more extensive set of PyAG point mutations. These include the changes UAG to AAG, GAG, UGG, UUG, UAU and UAC introduced in the context of the standard *ACT1-CUP1* gene fusion. The exon sequences of construct set II are different from those of set I in the region between the 3′ splice site and the *CUP1* coding sequence (Figure 2C, set II *vs.* set I). These were transformed into wild-type strains and *prp8-121–prp8-125* mutants and splicing was analyzed by primer extension and/or growth on copper-containing media (Tables 5 and 6). We divided the reporter constructs into two groups based on the severity of splicing defect that each causes and on the pattern of splicing each exhibits. For 3′ UAG (wild type), AAG, GAG and UGG, we observe splicing to only the correct 3′ splice site in both wild-type and mutant strains, and observe growth on copper-containing media above background levels. For 3′ UAG and AAG the levels of lariat intermediate produced are too low to accurately determine the (M/LI) ratio. For these two constructs, we only measured growth on copper-containing media. For 3′ GAG and UGG, we measured splicing by growth on copper-containing media and by primer extension.

For the wild-type *ACT1-CUP1* intron (3′ UAG), we observe a slight reduction in splicing efficiency in *prp8-121–prp8-125* strains compared with the wild-type strain (Figure 5A, lane 2 *vs.* lanes 3–7, Table 5). 3′ AAG is spliced equally well in wild-type strains and in *prp8-121–*

**TABLE 5**

**3′ splice site suppression with construct set II: 3′ UAG, AAG, GAG, UGG**

| | | Primer extension analysis | | Copper growth | |
|---|---|---|---|---|---|
| Strain | RNA | M/LI | Fold suppression | Copper growth (mM) | Fold suppression |
| *PRP8* | 3′ UAG (WT) | ND | NA | 2 | NA |
| *prp8-121* | 3′ UAG (WT) | ND | NA | 1.5 | None |
| *prp8-122* | 3′ UAG (WT) | ND | NA | 1.5 | None |
| *prp8-123* | 3′ UAG (WT) | ND | NA | 1.5 | None |
| *prp8-124* | 3′ UAG (WT) | ND | NA | 1.5 | None |
| *prp8-125* | 3′ UAG (WT) | ND | NA | 1.5 | None |
| *PRP8* | 3′ AAG | ND | NA | 1.5 | NA |
| *prp8-121* | 3′ AAG | ND | NA | 1.5 | None |
| *prp8-122* | 3′ AAG | ND | NA | 1.5 | None |
| *prp8-123* | 3′ AAG | ND | NA | 1.5 | None |
| *prp8-124* | 3′ AAG | ND | NA | 1.5 | None |
| *prp8-125* | 3′ AAG | ND | NA | 1.5 | None |
| *PRP8* | 3′ GAG | 1.8 | NA | ±0.18 | NA |
| *prp8-121* | 3′ GAG | 18 | 10× | 0.75 | 4× |
| *prp8-122* | 3′ GAG | 9.9 | 6× | 0.5 | 3× |
| *prp8-123* | 3′ GAG | 9.6 | 5× | 1 | 6× |
| *prp8-124* | 3′ GAG | 18 | 10× | 1 | 6× |
| *prp8-125* | 3′ GAG | 26 | 14× | 1 | 6× |
| *PRP8* | 3′ UGG | 1.1 | NA | 0.075 | NA |
| *prp8-121* | 3′ UGG | 11 | 10× | 0.5 | 7× |
| *prp8-122* | 3′ UGG | 4.1 | 4× | 0.18 | 2× |
| *prp8-123* | 3′ UGG | 8.7 | 8× | 0.75 | 10× |
| *prp8-124* | 3′ UGG | 7.6 | 7× | 0.25 | 3× |
| *prp8-125* | 3′ UGG | 6.7 | 6× | 0.25 | 3× |

See legend for Table 3.

*prp8-125* (Figure 5B, lanes 2–7; Table 5). The splicing block caused by the 3′ GAG construct is substantially suppressed in *prp8-121–prp8-125* strains. By growth on copper-containing media, the pattern of allele specificity is similar to that seen for 3′ GAG in construct set I, but the differences between *prp8-123–prp8-125* and *prp8-121–prp8-122* are less pronounced (Table 5). This difference is also reflected in the primer extension analysis (Figure 5C, lane 2 *vs.* lanes 3 and 4 and 5–7; Table 5). The exceptions are *prp8-121* and *prp8-123,* which have primer extension M/LI values that are higher and lower, respectively, than expected from growth on copper assays (Table 5). Since growth on copper-containing media itself is a reproducible measure of the amount of mature message produced, these results suggest that the mutants may also alter the stability of the lariat intermediate as a secondary phenotype and thus slightly skew the M/LI ratio. Although we include an internal standard (U1 snRNA labeled "control") in each primer extension experiment, the reproducibility between samples for U1 or other standards is approximately two- to threefold, whereas the M/LI ratio is highly reproducible between samples (usually <1.5-fold). Thus, the error introduced in trying to measure the amount of LI for each sample would be greater than the differences we wished to measure.

For 3′ UGG, we see a wide range of suppression on copper varying from twofold in *prp8-122* to 10-fold in *prp8-123* (Table 5). The results of primer extension analysis generally match the results from growth on copper assays but, again, vary somewhat due to the relative contributions of decreased lariat intermediate and increased mature message to the (M/LI) ratio (Figure 5D; Table 5). In summary, for wild-type and 3′ AAG, which display little or no splicing defect, we see no suppression. For 3′ splice site alterations that exhibit a strong splicing defect (3′ GAG and UGG), we see suppression by *prp8-123–prp8-125.*

*Construct set II (3′ UUG, UAU and UAC):* With 3′ UUG, UAU and UAC, we observe splicing to the correct 3′ splice site and to an upstream, cryptic 3′ splice site at position −5 in the intron. The sequence preceding the cryptic cleavage site is AUG/, as has been noted previously (PARKER and SILICIANO 1993). These constructs produce very little mature message in a wild-type strain and show growth on copper-containing media at or near background levels. Although we observe increased resistance to copper in *prp8-121–prp8-125* with 3′ UUG, AU and UAC (data not shown), the degree of suppression is difficult to assess by growth on copper-containing media since the starting resistances are not measurable and because the cryptic 3′ splice site is not in-frame with the *CUP1* coding sequence. Therefore, we used only primer extension to quantitate splicing of these

**TABLE 6**

**3′ splice site suppression with construct set II: 3′ UUG, UAU, UAC**

| Strain | RNA | $M_{Wt}/M_{cryptic}$ | Cryptic 3′ splice site usage | | Authentic 3′ splice site usage | |
|---|---|---|---|---|---|---|
| | | | $M_{crypt}$/LI | Fold suppression | $M_{Wt}$/LI | Fold suppression |
| *PRP8* | 3′ UUG | 0.78 | 0.018 | NA | 0.014 | NA |
| *prp8-121* | 3′ UUG | 1.0 | 0.15 | 8× | 0.15 | 11× |
| *prp8-122* | 3′ UUG | 0.44 | 0.11 | 6× | 0.048 | 3× |
| *prp8-123* | 3′ UUG | 1.2 | 0.10 | 6× | 0.13 | 9× |
| *prp8-124* | 3′ UUG | 1.1 | 0.081 | 5× | 0.087 | 6× |
| *prp8-125* | 3′ UUG | 0.98 | 0.096 | 5× | 0.094 | 7× |
| *PRP8* | 3′ UAU | 1.4 | 0.035 | NA | 0.049 | NA |
| *prp8-121* | 3′ UAU | 1.7 | 0.25 | 7× | 0.43 | 9× |
| *prp8-122* | 3′ UAU | 0.91 | 0.33 | 9× | 0.30 | 6× |
| *prp8-123* | 3′ UAU | 2.4 | 0.32 | 9× | 0.77 | 16× |
| *prp8-124* | 3′ UAU | 2.3 | 0.13 | 4× | 0.30 | 6× |
| *prp8-125* | 3′ UAU | 2.1 | 0.22 | 6× | 0.45 | 9× |
| *PRP8* | 3′ UAC | 0.21 | 0.21 | NA | 0.047 | NA |
| *prp8-121* | 3′ UAC | 0.47 | 0.66 | 3× | 0.31 | 7× |
| *prp8-122* | 3′ UAC | 0.30 | 0.67 | 3× | 0.21 | 4× |
| *prp8-123* | 3′ UAC | 0.82 | 0.36 | 2× | 0.30 | 6× |
| *prp8-124* | 3′ UAC | 0.69 | 0.19 | None | 0.13 | 3× |
| *prp8-125* | 3′ UAC | 0.49 | 0.21 | None | 0.099 | 2× |

The first and second columns indicate the strain and 3′ splice site reporter construct from set II. The third column is the ratio of wild-type ($M_{Wt}$) to cryptic ($M_{Crypt}$) mature message produced. The fourth and fifth columns show quantitation of the efficiency of cryptic 3′ splice site usage measured by the ratio of ($M_{Crypt}$) to lariat intermediate (LI) and compared with wild type to give fold suppression. The sixth and seventh columns show similar data for the wild-type 3′ splice site. NA, not applicable.

constructs. We measured three values: the efficiency of splicing to the wild-type 3′ splice site ($M_{wt}$/LI), the efficiency of cryptic 3′ splice site usage ($M_{crypt}$/LI) and the ratio of authentic to cryptic splice site usage ($M_{wt}/M_{cryptic}$).

The pattern of suppression of 3′ UUG in construct set II ($M_{wt}$/LI) is generally similar to what we observed for 3′ UUG of construct set I, with differences between alleles being less pronounced. The unexpectedly weak apparent suppression by *prp8-122* (threefold increase in M/LI) in this context may reflect an increase in the stability of the LI with this construct. In general, the allele specificity has been preserved for the two sets of constructs containing 3′ GAG and 3′ UUG alterations, but the levels of suppression are also clearly subject to modification by surrounding sequence context.

The overall pattern we see for 3′ UUG, 3′ UAU and 3′ UAC in *prp8-121-prp8-125* is suppression of both the authentic and cryptic splice sites in the mutant strains (Figure 6, A–C, lane 2 *vs.* lanes 3–7; Table 6). The authentic 3′ splice site is usually suppressed slightly better than the cryptic 3′ splice site but not always. For example, the *prp8-122* strain suppresses cryptic splicing of 3′ UUG and 3′ UAU better than it suppresses authentic splicing (Figure 6, A and B, lane 2 *vs.* 4; Table 6). With 3′ UAC, suppression values in Table 6 appear lower than what is visualized in the primer extension experiment (Figure 6C, lane 2 *vs.* lanes 3–7) because the wild-type sample (lane 2) is underloaded and because the mutants may stabilize the LI compared to wild type.

The ratio of authentic to cryptic splice site usage ($M_{wt}/M_{cryptic}$) is useful for evaluating the *prp8-121–prp8-125* strains since it gives a measure of relative preference for two competing 3′ splice sites. This ratio is altered substantially in some of the mutant strains. For example the ratio changes fourfold in favor of the authentic 3′ splice site with 3′ UAC in a *prp8-123* strain. In contrast, ($M_{wt}/M_{cryptic}$) changes twofold in favor of the cryptic 3′ splice site in *prp8-122* with 3′ UUG (Table 6). In general, the deviations in ($M_{wt}/M_{cryptic}$) for the mutant strains support the notion that these alleles cause altered recognition of the 3′ splice site.

*3′ splice site alteration in a heterologous intron:* Because surrounding sequence context has some effect on suppression (cf 3′ UUG and 3′ GAG; Tables 3, 5 and 6), we wished to determine whether the 3′ splice site suppression we observed with actin intron constructs would also be observed in the novel context of a different intron. We used an *rp51a-lacZ* fusion construct with a mutant 3′ splice site (UGG) to address this question (CHANFREAU *et al.* 1994). The splicing of this construct is suppressed between 1.2- and 15-fold when assayed in *prp8-121–prp8-125* strains, indicating that suppression is not intron specific (Table 4). Thus, these alleles of *PRP8* do not require a specific surrounding sequence context to suppress PyAG alterations at the 3′ splice site.

In summary, *prp8-121–prp8-125* demonstrate several interesting properties: they suppress the effects of point mutations in the 3′ splice site but not the effects of mutations elsewhere in the intron; 3′ splice site suppression is not specific for any particular point mutation in

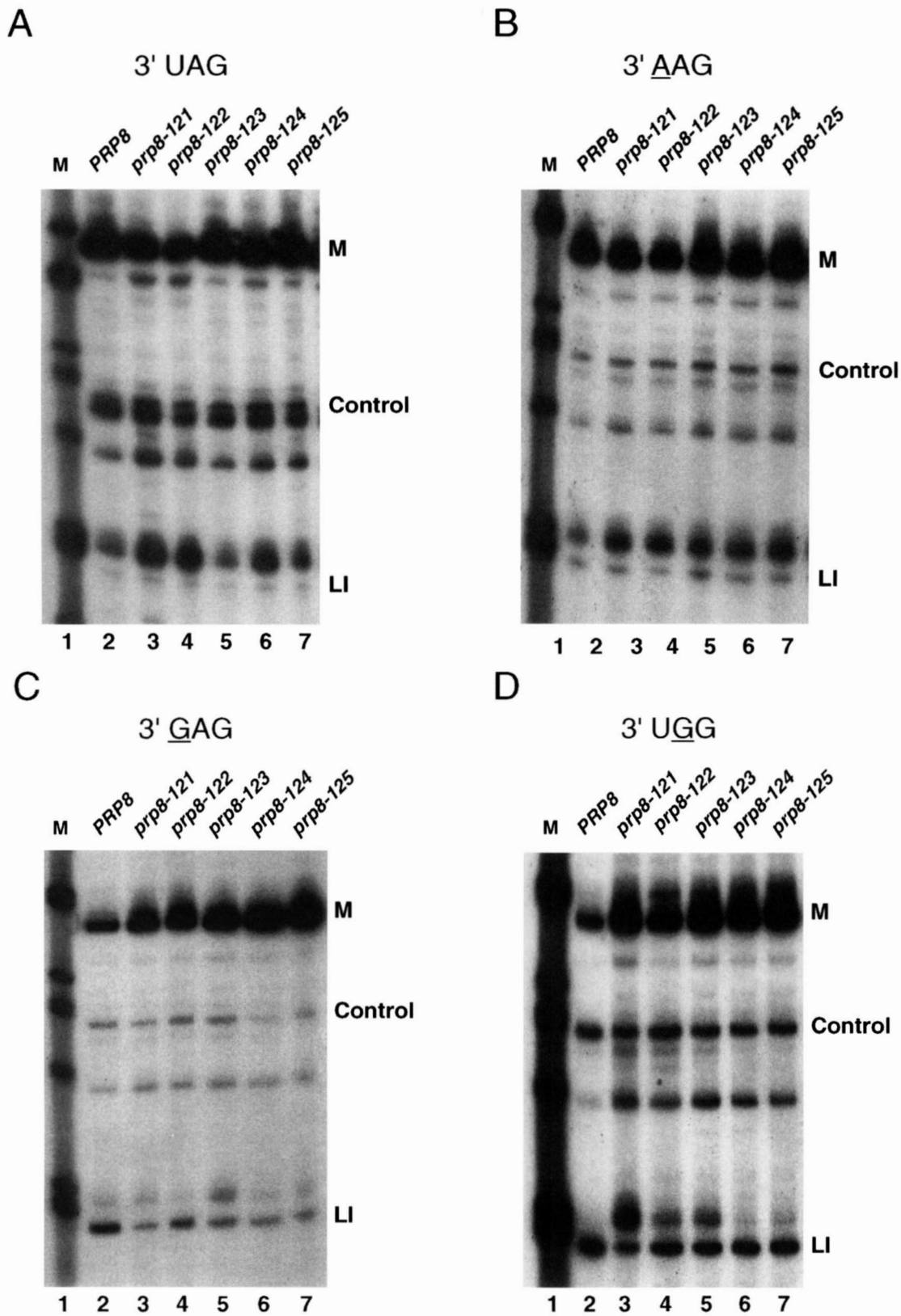


FIGURE 5.—Splicing of 3′ splice site mutant construct set II. (A–D) Primer extension analysis of splicing to 3′ UAG (wt intron), AAG, GAG and UGG. Gels are marked as in Figure 4.

the PyAG motif, but the alleles display a complex pattern of preferences; the preferences displayed by the alleles preclude ordering them into an allelic series based on relative strength of suppression; the suppression phenotype can be partially altered by surrounding sequence context, as evidenced by differences between construct set I and II; however, a specific sequence context is not necessary for suppression.

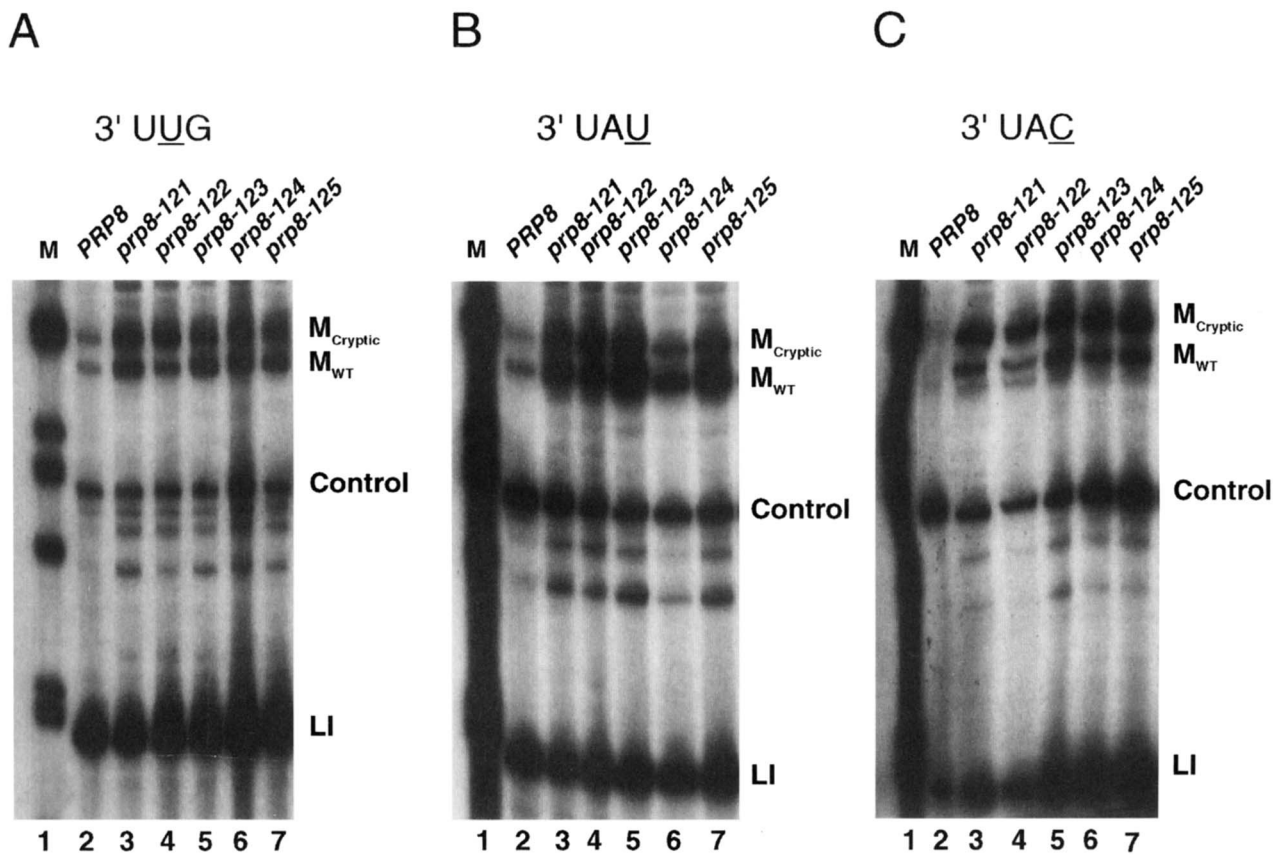


FIGURE 6.—Splicing of 3′ splice site mutant construct set II. (A) Primer extension analysis of splicing to 3′ splice site mutant UUG in wild-type (lane 2) and *prp8-121–prp8-125* (lanes 3–7) strains. Primer extension products corresponding to mature message from use of the authentic 3′ splice site ($M_{WT}$) or cryptic 3′ splice at position −5 ($M_{Cryptic}$), lariat intermediate (LI) or U1 snRNA internal control (control) are marked next to the gel. Lane 1 (marked M) contains size markers (*Hpa*II-digested pBR325). (B and C) Primer extension analysis of splicing to 3′ UAU and UAC. Lanes and primer extension products are marked as in (A).

**Mapping 3′ splice site fidelity mutations:** To determine the identity of the mutations in *prp8-121–prp8-125,* we first used gap repair to map the region of *PRP8* that contained the relevant change. We then sequenced a 1.2-kb *Bst*BI-*Cla*I fragment from region C that was predicted to contain the relevant alteration for each allele. In each case, this region was found to contain one or more missense mutations (Table 7). *prp8-122* and *prp8-124* have single alterations in this fragment whereas *prp8-121, -123* and *-125* encode multiple changes.

To determine whether or not these changes were sufficient to elicit the observed suppression phenotype, we used a similar strategy as that employed for the *prp8-101*-like alleles. The cloned *1.2-kb Bst*BI-*Cla*I fragment from each allele and from wild type was amplified using PCR under nonmutagenic conditions. This DNA was then cotransformed with a *PRP8* plasmid that had been partially cut with *Bst*EII. One of two *Bst*EII sites in the *PRP8* gene lies in the middle of the cloned region (see MATERIALS AND METHODS). In each case, the cotransformed PCR fragment from the mutant allele generated a suppressor phenotype at a rate >100-fold higher than that of cotransformed wild-type PCR DNA. The *prp8-124* PCR DNA generated suppressors at a frequency only 10-fold above wild type, but this result was expected since the mutation on this fragment lies much farther from the *Bst*EII site than the changes in the other alleles.

Since *prp8-121, -123* and *-125* each contain more than one mutation, it was of interest to know which alteration(s) is responsible for the suppression phenotype. We took advantage of the fact that there is at least one mutation in each of these alleles on either side of the aforementioned *Bst*EII site. Reciprocal swaps were constructed that contained all six possible wild-type/mutant or mutant/wild-type combinations of parent vector and heterologous 2.1 kb *Bst*EII fragment. In each case, a single mutation was isolated and found to be responsible for the phenotype (Table 7; Figure 7). Four of the suppressor mutations alter amino acids in a region of 44 residues spanning positions 1565–1609. The fifth, in *prp8-124,* alters an amino acid 166 residues N-terminal to this stretch.

## DISCUSSION

Several studies have shown that Prp8p interacts with intron sequences that are critical for splicing (WYATT *et al.* 1992; TEIGELKAMP *et al.* 1995; UMEN and GUTHRIE

**TABLE 7**

**Mutations in PRP8 identified in this study**

| *PRP8* allele | Mutation(s) | No. isolates |
|---|---|---|
| *prp8-101* | **E1960K** | 2 |
| *prp8-102* | **E1960G** | 3 |
| *prp8-103* | **F1834L,** V1946A | 1 |
| *prp8-104* | **F1834S,** R1922G | 1 |
| *prp8-105* | **F1834L,** F1880S | 1 |
| *prp8-106* | **F1834S** | 1 |
| *prp8-107* | **F1834L** | 2 |
| *prp8-121* | **W1609R,** N1618D | 1 |
| *prp8-122* | **W1575R** | 1 |
| *prp8-123* | **E1576V,** S1705C[a], N1730Y[a] | 1 |
| *prp8-124* | **M1399I** | 1 |
| *prp8-125* | **T1565A,** N1721Y, V1752A | 1 |

The first column indicates the allele designation for each *PRP8* mutation. The second column indicates the mutations found by sequencing regions of each mutant. The alteration responsible for the selected phenotype with each allele is in bold. The number of isolates containing each mutation is shown in column three.

[a] These two mutations give weak 3′ splice site suppression when present without the E1576V alteration. However, the E1576V change alone is sufficient to give the full level of 3′ splice suppression seen in the original *prp8-123* isolate.

1995a). Furthermore, the large size (280 kD) and sequence conservation of Prp8p suggest that it mediates multiple interactions with spliceosomal RNAs and proteins (ANDERSON *et al.* 1989; PINTO and STEITZ 1989; HODGES *et al.* 1995). However, it has been difficult to assess the functional significance of these interactions. Removal of Prp8p by heat inactivation of a temperature-sensitive allele or by *in vivo* depletion reveals a role for the protein in maintaining the integrity of the U4/U5/U6 triple snRNP (BROWN and BEGGS 1992). Since the U4/U5/U6 snRNP is required during spliceosome assembly, however, these methods cannot be used to assess the function(s) of Prp8p within the spliceosome.

**Uridine tract recognition by Prp8p:** By repeating our original search for uridine tract recognition mutants using a mutagenized *PRP8* library, we have isolated six new alleles of *PRP8* that contain alterations in one of two amino acids, E1960 and F1834. As mutations in these amino acids were isolated multiple times, it appears that we have saturated this search, at least for single changes that yield a strong uridine tract recognition phenotype. Notably, none of the new alleles isolated are significantly stronger in phenotype than *prp8-101,* and all are haploviable. It is possible that alleles of *PRP8* exist that change the ratio of splice site usage even more than the ones we isolated but do not result in a net increase in usage of the adenosine-rich 3′ splice site. However, one observation argues that the alleles we isolated are the most severe that could be recovered from this screen. The ratios of proximal to distal splice site usage for +T PyDOWN in our mutant strains is similar to the ratio of splice site usage in a wild-type strain when no uridine tract precedes either 3′ splice site in a *cis* competition (PATTERSON and GUTHRIE 1991). Thus, *prp8-101-prp8-107* behave as though there were no uridine tract preceding the proximal 3′ splice site in +T PyDOWN.

It is clear from this work that only a very limited and specific set of changes in *PRP8* leads to loss of uridine preference. Residue 1834 contains a conservative change from F to Y in *Caenorhabditis elegans,* and residue 1960 is conserved as an E in *Saccharomyces cerevisiae, Caenorhabditis elegans, Homo sapiens,* and *Oryza sativa* (HODGES *et al.* 1995) (Figure 7). It is important to bear in mind that we selected and characterized only the strongest uridine recognition alleles of *PRP8.* The weaker alleles that we did not characterize were also isolated from the C and D libraries and probably lie in the same region of overlap. Supporting this idea, changes in positions 1880, 1922 and 1946 occur along with changes in position 1834 in *prp8-103–prp8-105,* and these additional changes cause some alteration in the phenotype (Tables 2 and 7). Thus, the region encompassing residues 1834–1960 of Prp8p is likely to be involved in uridine tract recognition. Until a larger number of weaker alleles are mapped, we cannot precisely define the limits of this functional domain. Nonetheless, we have identified the key amino acids in Prp8p, E1960 and F1834, that make the largest contribution to uridine tract recognition. These residues are predicted to function either through direct contact with the uridine tract or by stabilizing a structure in Prp8p that binds this sequence. Supporting the idea that residue 1960 facilitates uridine tract binding by Prp8p is our observation that the E1960K mutation, *prp8-101,* causes a decrease in crosslinking of Prp8p to the 3′ splice site *in vitro* (UMEN and GUTHRIE 1995b).

**Prp8p governs the fidelity of 3′ splice site usage:** Because Prp8p might be present at or near the active site during the second catalytic step, we wished to determine whether this protein is involved in recognition of the PyAG nucleotides that directly precede the reactive phosphate at the 3′ splice junction. The PyAG motif is known to be critical for proper 3′ splice site recognition and utilization (REED and MANIATIS 1985; RUSKIN and GREEN 1985; VIJAYRAGHAVAN *et al.* 1986; FOUSER and FRIESEN 1987; REED 1989; PARKER and SILICIANO 1993; CHANFREAU *et al.* 1994). In this work, we have identified five new alleles of *PRP8* that suppress the inhibitory effects of PyAG alterations at the 3′ splice site. This phenotype markedly contrasts that displayed by the uridine tract recognition mutant *prp8-101,* which strongly exacerbates the splicing defect of PyAG alterations (UMEN and GUTHRIE 1995a). Moreover, the PyAG suppressor alleles *prp8-121–prp8-125* do not show a defect in uridine tract recognition, nor do they suppress alterations at the branchsite. Three of the five alleles, *prp8-121, -122* and *-124* actually exacerbate the effects of mutations at both the branchsite and 5′ splice site. *prp8-123* and *prp8-125* have no effect on splicing of the

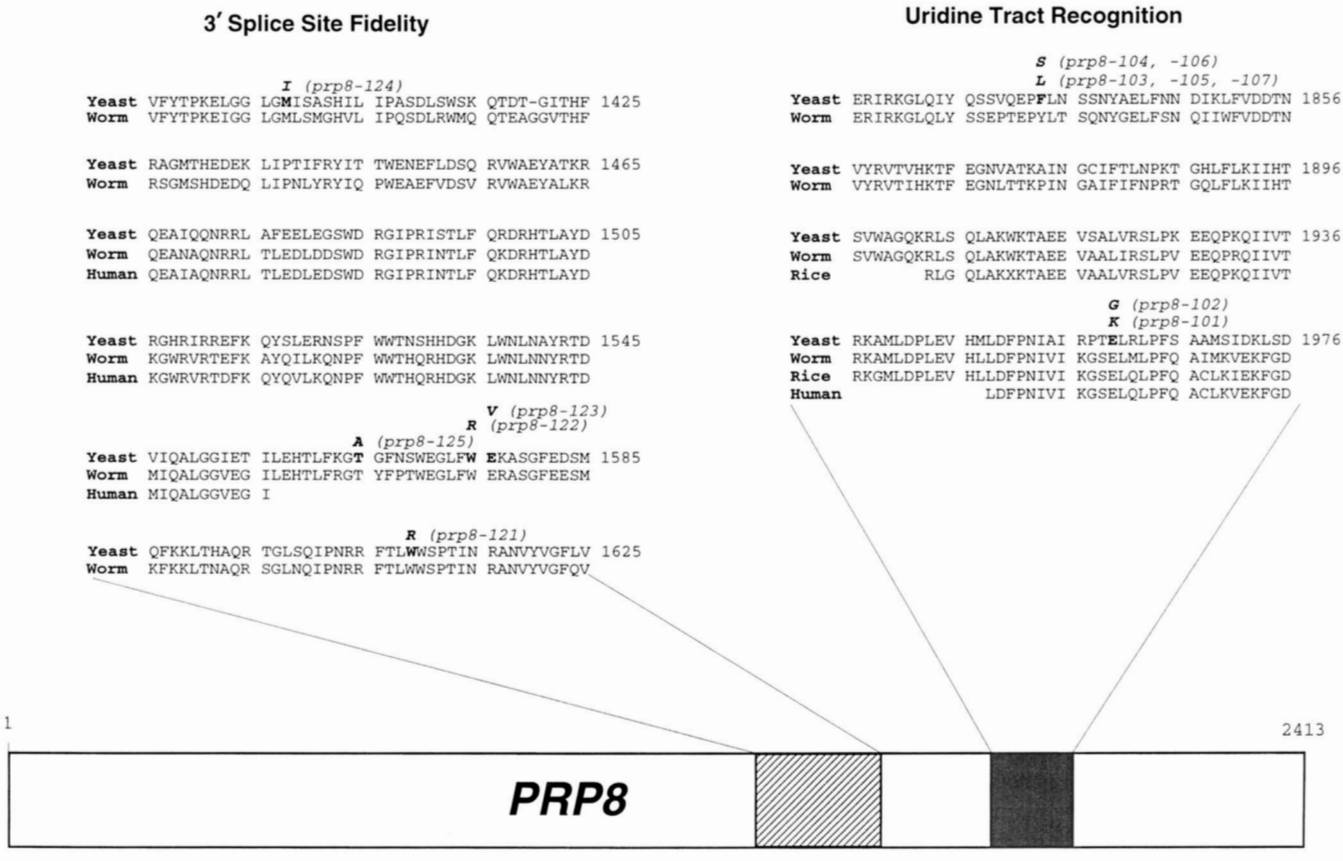


FIGURE 7.—Domains of *PRP8* involved in uridine tract recognition and in maintaining the fidelity of 3′ splice site usage. The bottom shows a schematic of Prp8, length 2413 amino acids. The hatched box shows the region where 3′ splice site fidelity mutants are located and the gray box shows the location of uridine tract recognition mutants. These regions are expanded to show the location of the relevant change for each allele (see Table 7 for locations of other alterations). The nature of the mutation for each allele is shown in bold above the wild-type residue. Included is an alignment with portions of *PRP8* homologues from other species: *C. elegans* (worm), *H. sapiens* (human) and *O. Sativa* (rice) (Hodges *et al.* 1995). The numbering on the right reflects the position in the yeast sequence.

branchsite mutant we tested, and with a 5′ splice site mutation, show very weak suppression of either aberrant or normal 5′ splice site cleavage. It is possible that this weak 5′ splice site suppression results from the secondary mutations associated with *prp8-123* and *prp8-125*. In any case, weak 5′ splice site suppression is not obligatorily coupled to 3′ splice site suppression since other 3′ splice site suppressor mutants do not display this phenotype. Finally, the suppressors function in the context of a heterologous intron with a 3′ splice site mutation. Thus, these alleles are specific in their suppression of PyAG mutations and functionally distinct from the alleles which affect uridine tract recognition (Table 4).

*prp8-121–prp8-125* were selected using two different PyAG variants, GAG and UUG (Table 3). In principle, suppression of 3′ splice site mutations by these alleles of *PRP8* could occur by an indirect mechanism. For example, if these alleles alter a kinetic parameter that affects fidelity of 3′ splice site usage, we might expect to see similar suppression for all 3′ splice site mutants, or an allelic series where some alleles always generate higher levels of suppression than others. An example of an indirect mechanism is suppression of branchsite alterations by mutations in *PRP16*, which encodes an RNA-dependent ATPase (BURGESS *et al.* 1990; SCHWER and GUTHRIE 1991). The *PRP16* suppressor alleles affect the ATPase activity of the protein, and there is a correlation between strength of suppression and reduction in ATPase activity (BURGESS and GUTHRIE 1993). The mechanism of suppression is indirect, in the sense that it does not require altered recognition of aberrant branchsites by Prp16p. Instead, the slowed ATPase activity of the mutant proteins allows more time for aberrant branch lariats, which would otherwise be degraded, to continue productively in the splicing pathway (BURGESS and GUTHRIE 1993).

In contrast to branchsite suppressor alleles of *PRP16*, the 3′ splice site suppressor alleles of *PRP8* cannot be placed into an allelic series based on strength of suppression. Instead, these alleles show a complex pattern of specificity with different 3′ splice sites. Most illustrative of this specificity are the two 3′ splice site alterations with which these *PRP8* alleles were selected, 3′ GAG and 3′ UUG. *prp8-121* and *prp8-122* suppress the 3′ UUG alteration much better than they suppress 3′ GAG, and *prp8-123*, *-124* and *-125* suppress 3′ GAG much better

than they suppress 3′ UUG (Table 3). For other constructs, the matrix of suppression is more complicated and does not form a predictable pattern. Thus, the suppression we observe is difficult to explain via a completely indirect mechanism.

If these *PRP8* alleles do not act indirectly, how might they alter the fidelity of 3′ splice site selection? The simplest possibility is that Prp8p makes direct contact with the PyAG trinucleotide and surrounding sequences to form part of a 3′ splice site binding site. This idea is supported by the fact that Prp8p can be crosslinked to the 3′ splice site during the second catalytic step (TEIGELKAMP *et al.* 1995; UMEN and GUTHRIE 1995b). Mutant Prp8p would be predicted to bind altered 3′ splice sites with less discrimination than the wild-type protein and allow these substrates to be utilized at a higher rate.

It is especially intriguing that mutations in two spliceosomal snRNAs, U2 A25 and U6 G52 also suppress PyAG alterations (LESSER and GUTHRIE 1993b; MADHANI and GUTHRIE 1994). These two nucleotides are thought to participate in a tertiary interaction that forms part of the active site for the second catalytic step (MADHANI and GUTHRIE 1994). Moreover, the 3′ splice site suppression we see for *prp8-121–prp8-125* appears to be stronger and more specific than that seen for the snRNA mutations. Therefore, if *prp8-121–prp8-125* do not alter a direct interaction between Prp8p and the 3′ splice site, then these alleles are likely to alter the geometry of the active site in such a way as to relax the specificity normally imposed on 3′ splice site nucleotide identity. This kind of phenotype has been previously documented for active site mutations in alpha-lytic protease that broaden substrate specificity. These alpha-lytic protease mutations cause increased flexibility in the active site, which allows a larger spectrum of amino acid side chains to be accommodated (BONE *et al.* 1991).

Notably, the alterations in *PRP8* that lead to strong 3′ splice site suppression all cluster in a relatively small region of the protein. The changes we identified are also in residues that are conserved between yeast and worms. Four of the five alterations are in a 44 amino acid stretch, and the fifth change lies 166 residues towards the N-terminus from this stretch (Figure 7). The clustering suggests that this region of the protein may make critical contacts with the 3′ splice site or active site residues. Since we found weaker suppressors in other regions of the protein, other types of structural perturbations may also alter the interaction of Prp8p with the 3′ splice site. However, it should be emphasized that 3′ splice site suppressors appear at a relatively low frequency. Moreover, general loss of function mutations, such as the temperature sensitive mutants we isolated in this study, do not affect 3′ splice site utilization (Table 1; UMEN and GUTHRIE 1995a).

The two types of 3′ splice site utilization mutants we isolated in this study are located relatively close to one another within the primary sequence of Prp8p (Figure 7). It is, therefore, tempting to speculate that this region of the protein functions in 3′ splice site selection. However, structural data and more extensive genetic mapping are required to determine whether this 561 amino acid region of the protein also carries out other functions. In any event, our findings should provide a useful guide for future analysis aimed at a more detailed biochemical and structural understanding of how Prp8p interacts with the 3′ splice site.

The mutagenized *PRP8* library we have constructed, in combination with sensitive genetic assays, has proven useful in dissecting the roles of Prp8p in the spliceosome and also in defining specific functional domains. Although we have focused our studies on 3′ splice site selection and the second catalytic step of splicing, this library has many other potential uses. For example, it is now being employed to find alterations that influence the fidelity of 5′ splice selection (AMY KISTLER, personal communication). The library could also be used to examine the interactions of Prp8p with snRNAs and spliceosomal proteins. Recently, we have put *PRP8* under the control of a regulated promoter to enable a screen for dominant negative alleles. This class of allele will be particularly useful in identifying new functions for Prp8p.

We thank CATHY COLLINS, IRA HERSKOWITZ, AMY KISTLER and PRATIMA RAGHUNATHAN for critical comments on this manuscript. We are grateful for the excellent technical assistance provided by LUCITA ESPERAS, CAROL PUDLOW and HELI ROIHA. We thank AMY KISTLER for the G5A reporter constructs used for screening mutants. This work was supported by a National Institutes of Health (NIH) training grant and a National Science Foundation predoctoral fellowship to J.G.U. and NIH research grant GM-21119 to C.G. C.G. is an American Cancer Society Research Professor of Molecular Genetics.

## LITERATURE CITED

ANDERSON, G. J., M. BACH, R. LUHRMANN and J. D. BEGGS, 1989 Conservation between yeast and man of a protein associated with U5 small nuclear ribonucleoprotein. Nature **342:** 819–821.

BONE, R., A. FUJISHIGE, C. A. KETTNER and D. A. AGARD, 1991 Structural basis for broad specificity in alpha-lytic protease mutants. Biochemistry **30:** 10388–10398.

BROWN, J. D., and J. D. BEGGS, 1992 Roles of PRP8 protein in the assembly of splicing complexes. EMBO J. **11:** 3721–3729.

BURGESS, S. M., and C. GUTHRIE, 1993 A mechanism to enhance mRNA splicing fidelity: the RNA-dependent ATPase Prp16 governs usage of a discard pathway for aberrant lariat intermediates. Cell **73:** 1377–1391.

BURGESS, S., J. R. COUTO and C. GUTHRIE, 1990 A putative ATP binding protein influences the fidelity of branchpoint recognition in yeast splicing. Cell **60:** 705–717.

CHANFREAU, G., P. LEGRAIN, B. DUJON and A. JACQUIER, 1994 Interaction between the first and last nucleotides of pre-mRNA introns is a determinant of 3′ splice site selection in S. cerevisiae. Nucleic Acids Res. **22:** 1981–1987.

DEIRDRE, A., J. SCADDEN and C. W. SMITH, 1995 Interactions between the terminal bases of mammalian introns are retained in inosine-containing pre-mRNAs. EMBO J. **14:** 3236–3246.

FOUSER, L. A., and J. D. FRIESEN, 1987 Effects on mRNA splicing of mutations in the 3′ region of the Saccharomyces cerevisiae actin intron. Mol. Cell. Biol. **7:** 225–230.

FRANK, D., and C. GUTHRIE, 1992 An essential splicing factor, SLU7, mediates 3′ splice site choice in yeast. Genes Dev. **6:** 2112–2124.

GOZANI, O., J. G. PATTON and R. REED, 1994 A novel set of spliceosome-associated proteins and the essential splicing factor PSF

bind stably to pre-mRNA prior to catalytic step II of the splicing reaction. EMBO J. **13:** 3356–3367.

GREEN, M. R., 1991 Biochemical mechanisms of constitutive and regulated pre-mRNA splicing. Annu. Rev. Cell Biol. **7:** 559–599.

GUTHRIE, C., 1991 Messenger RNA splicing in yeast: clues to why the spliceosome is a ribonucleoprotein. Science **253:** 157–163.

GUTHRIE, C., and G. R. FINK, 1991 *Guide to Yeast Genetics and Molecular Biology.* Academic Press, San Diego.

HODGES, P. E., S. P. JACKSON, J. D. BROWN and J. D. BEGGS, 1995 Extraordinary sequence conservation of the PRP8 Splicing Factor. YEAST **11:** 337–342.

JACKSON, S. P., M. LOSSKY and J. D. BEGGS, 1988 Cloning of the RNA8 gene of Saccharomyces cerevisiae, detection of the RNA8 protein, and demonstration that it is essential for nuclear pre-mRNA splicing. Mol. Cell. Biol. **8:** 1067–1075.

LESSER, C. F., and C. GUTHRIE, 1993a Mutational analysis of pre-mRNA splicing in *Saccharomyces cerevisiae* using a sensitive new reporter gene, CUP1. Genetics **133:** 851–863.

LESSER, C. F., and C. GUTHRIE, 1993b Mutations in U6 snRNA that alter splice site specificity: implications for the active site. Science **262:** 1982–1988.

LEUNG, D. W., E. CHEN and D. V. GOEDDEL, 1989 A method for random mutagenesis of a defined DNA segment using a modified polymerase chain reaction. Technique **1:** 11–15.

MADHANI, H. D., and C. GUTHRIE, 1994 Randomization-selection analysis of snRNAs in vivo: evidence for a tertiary interaction in the spliceosome. Genes Dev. **8:** 1071–1086.

MANIATIS, T., E. F. FRITSCH and J. SAMBROOK, 1982 *Molecular Cloning: A Laboratory Manual.* Cold Spring Harbor Laboratory, Cold Spring Harbor, NY.

MILLER, J., 1972 In *Experiments in Molecular Genetics,* Cold Spring Harbor Laboratory Press, Cold Spring Harbor, NY.

MOORE, M. J., C. C. QUERY and P. A. SHARP, 1993 Splicing of precursors to mRNA by the spliceosome, pp. 303–358 in *The RNA World,* edited by R. F. GESTELAND and J. F. ATKINS. Cold Spring Harbor Laboratory Press, Cold Spring Harbor, NY.

MUHLRAD, D., R. HUNTER and R. PARKER, 1992 A rapid method for localized mutagenesis of yeast genes. Yeast **8:** 79–82.

NEWMAN, A. J., and C. NORMAN, 1992 U5 snRNA interacts with exon sequences at 5′ and 3′ splice sites. Cell **68:** 743–754.

PARKER, R. and C. GUTHRIE, 1985 A point mutation in the conserved hexanucleotide at a yeast 5′ splice junction uncouples recognition, cleavage, and ligation. Cell **41:** 107–118.

PARKER, R. and P. G. SILICIANO, 1993 Evidence for an essential non-Watson-Crick interaction between the first and last nucleotides of a nuclear pre-mRNA intron. Nature **361:** 660–662.

PATTERSON, B., and C. GUTHRIE, 1991 A U-rich tract enhances usage of an alternative 3′ splice site in yeast. Cell **64:** 181–187.

PATTON, J. G., E. B. PORRO, J. GALCERAN, P. TEMPST and G. B. NADAL, 1993 Cloning and characterization of PSF, a novel pre-mRNA splicing factor. Genes Dev. **7:** 393–406.

PIKIELNY, C. W., and M. ROSBASH, 1985 mRNA splicing efficiency in yeast and the contribution of nonconserved sequences. Cell **41:** 119–126.

PINTO, A. L., and J. A. STEITZ, 1989 The mammalian analogue of the yeast PRP8 splicing protein is present in the U4/5/6 small nuclear ribonucleoprotein particle and the spliceosome. Proc. Natl. Acad. Sci. USA **86:** 8742–8746.

REED, R., 1989 The organization of 3′ splice-site sequences in mammalian introns. Genes Dev. **3:** 2113–2123.

REED, R., and T. MANIATIS, 1985 Intron sequences involved in lariat formation during pre-mRNA splicing. Cell **41:** 95–105.

RUSKIN, B., and M. R. GREEN, 1985 Role of the 3′ splice site consensus sequence in mammalian pre-mRNA splicing. Nature **317:** 732–734.

RYMOND, B., and M. ROSBASH, 1992 Yeast pre-mRNA splicing, pp. 143–192 in *The Molecular and Cellular Biology of the Yeast Saccharomyces,* edited by E. W. JONES, J. R. PRINGLE and J. R. BROACH. Cold Spring Harbor Laboratory Press, Cold Spring Harbor, NY.

SCHWER, B., and C. GUTHRIE, 1991 PRP16 is an RNA-dependent ATPase that interacts transiently with the spliceosome. Nature **349:** 494–499.

SIKORSKI, R. S., and P. HIETER, 1989 A system of shuttle vectors and yeast host strains designed for efficient manipulation of DNA in *Saccharomyces cerevisiae.* Genetics **122:** 19–27.

SONTHEIMER, E. J., and J. A. STEITZ, 1993 The U5 and U6 small nuclear RNAs as active site components of the spliceosome. Science **262:** 1989–1996.

TEIGELKAMP, S., A. J. NEWMAN and J. D. BEGGS, 1995 Extensive interactions of PRP8 protein with the 5′ and 3′ splice sites during splicing suggest a role in stabilization of exon alignment by U5 snRNA. EMBO J. **14:** 2602–2612.

UMEN, J. G., and C. GUTHRIE, 1995a A novel role for a U5 snRNP protein in 3′ splice site selection. Genes Dev. **9:** 855–868.

UMEN, J. G., and C. GUTHRIE, 1995b Prp16p, Slu7p and Prp8p interact with the 3′ splice site in two distinct stages during the second catalytic step of pre-mRNA splicing. RNA **1:** 584–597.

VIJAYRAGHAVAN, U., R. PARKER, J. TAMM, Y. IIMURA, J. ROSSI *et al.,* 1986 Mutations in conserved intron sequences affect multiple steps in the yeast splicing pathway, particularly assembly of the spliceosome. EMBO J. **5:** 1683–1695.

WYATT, J. R., E. J. SONTHEIMER and J. A. STEITZ, 1992 Site-specific cross-linking of mammalian U5 snRNP to the 5′ splice site before the first step of pre-mRNA splicing. Genes Dev. **6:** 2542–2553.

ZAMORE, P. D., and M. R. GREEN, 1991 Biochemical characterization of U2 snRNP auxiliary factor: an essential pre-mRNA splicing factor with a novel intranuclear distribution. Embo J. **10:** 207–214.

Communicating editor: M. JOHNSTON